Realization of an end-to-end software simulator for navigation systems

J. Furthner*,†, E. Engler, A. Steingass, M. Angermann, J. Hahn, A. Hornbostel,
R. Krämer, H. P. Müller, T. Noack, P. Robertson, S. Schlüter and J. Selva

German Aerospace Center, D-82234 Wessling, Germany

SUMMARY

The paper presents the DLR-NAVSIM tool. This tool was developed for simulating future civil navigation satellite systems like GNSS-2 or Galileo. In the introduction the aim, the problems, and the principal set-up of the simulation tool are described. In Section 2 a detailed description of the two different levels is presented. Also described are the mean influences on a navigation system, which are realized within this tool in one of the two levels. Section 3 depicts some preliminary results of each level simulation to demonstrate the capacity of the DLR-NAVSIM tool for navigation satellite systems. Copyright © 2000 John Wiley & Sons, Ltd.

KEY WORDS: global navigation satellite system; GNSS; navigation; ionosphere; troposphere

1. INTRODUCTION

In the last few years the need for simulation tools for navigation systems has greatly increased. The problem of simulating navigation systems is, on the one hand, the handling of the large physical transmission bandwidth which causes a very high sampling frequency and computational complexity and, on the other hand, the comparatively slowly changing scenario (ionospheric or tropospheric influences, satellite tracks, user movements, clock drifts, and others). This conflict of time-scales would normally result in an extensive simulation effort which is not acceptable since it would lead to excessively long simulation times. In this paper we will present a multi-layer approach which ensures sufficiently the detailed description of the physical layer and still handles simulations over long periods of time.

* Correspondence to: J. Furthner, German Aerospace Centre, Institute of Communication and Navigation, DLR Oberpfaffenhofen, Münchner Str. 20, D-82234, Wessling, Germany.
† E-mail: johann.furthner@dlr.de

In the first step we create a simulation system for the physical layer. This signal simulation system operates on the signal level and allows for the investigation of signal structures (e.g. spreading codes, pulse shaping, chip rates) and corresponding design of signal generation and receiver components (e.g. HPA, DLL, PLL). Based on these simulations, where essential transmission impacts like multipath are considered, the system performance will be derived using (for example) 30 s long signal sections for a reasonable number of carrier-to-noise ratios C/No (CNR) for the considered multipath channel. Owing to the highly detailed simulation at sampling frequencies of 100 MHz and more, and the high computational complexity of interpolation and correlation, each of these 30 s real-time simulations take about one day on a high-performance workstation. The result of the simulation is a recording of the tracking error of the receiver loops, from which (amongst others) the variance, mean, and spectrum of the loop errors for each C/No-channel combination are extracted. In a second step a model of the physical signal processing for the system layer is generated based on these statistical parameters and on the noise-free dynamic behaviour (tracking error) of the DLL and PLL.

In a third step the comparatively slowly changing system aspects are modelled: Satellite tracks, user movements, atmospheric distortions (ionosphere, troposphere, channel selection), antenna effects, system and satellite time behaviour and importantly the solution of the navigation equation. This simulation system is, on the one hand, used to estimate the states of GNSS signals as characterized by CNR, ranges, phases and corresponding rates, and to derive representative samples for the detailed simulation. On the other hand, the corresponding delay measurements are composed (adding technical and natural/physical components) and used for positioning. This can be done for a specified number of dynamic or static users inside a defined region using one or several satellite systems. In this (upper) layer we are also able to test new algorithms such as navigation equation solvers, ionospheric estimation algorithms, intelligent directive antennas, clock models and others.

Since we use a flexible software and block-based design we can quickly adapt to changes of the system during the definition phase of GNSS2. The assessment of an overall system constellation can then be done by measuring the accuracy, the availability and even the reliability. By splitting the overall simulation task into these two layers and by employing the concept of error signal modelling, we are able to successfully tackle the problem of hugely different simulation time-scales.

The paper is organized as follows: we begin by presenting the architecture of the simulation system and its separation into the upper application simulation level (ASL) and the lower signal simulation level (SSL). This is followed by (preliminary) simulation results and sample plots of interesting physical system quantities for a specific date and location in Europe. The paper summarizes the main results of our work in a brief conclusion.

2. ARCHITECTURE OF THE SIMULATION SYSTEM

2.1. *Functional diagram*

The **NavSim** software simulation system consists of two levels: the signal simulation level (SSL) and the application simulation level (ASL). Both levels (Figure 1) are necessary to determine the positioning performance of a global navigation satellite system (GNSS) under consideration of nearly realistic conditions.
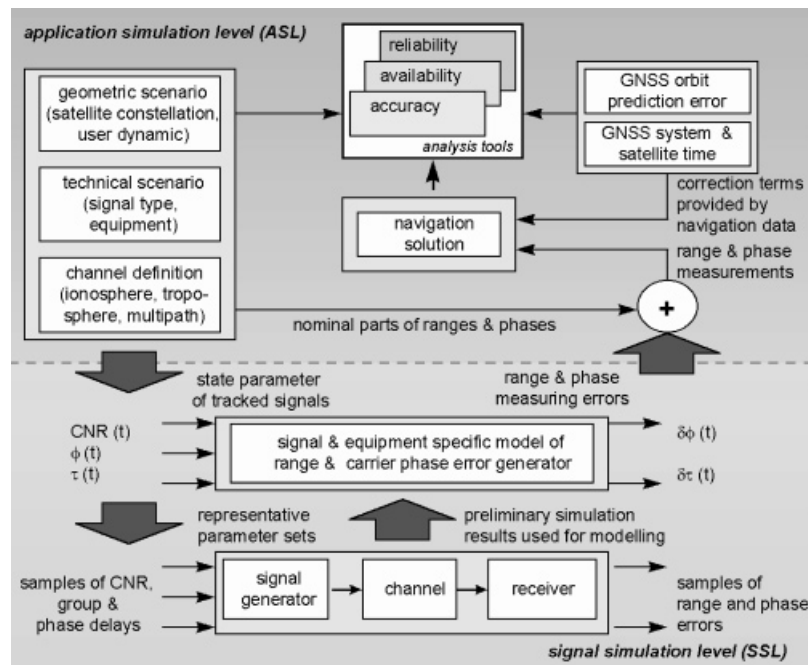
Figure 1. Functional diagram of the GNSS end-to-end software simulation system.

The application simulation level includes the control unit of the whole simulation system. This control unit is responsible, on the one hand, for the specification of the global simulation parameter like start and end points of simulation, considered region and sampling frequencies, and, on the other hand, it is responsible for the simulation system composition. The latter comprises the selection of optional modules and, therefore, the definition of the operation mode for the desired simulation tasks. Four basic types of operation mode are supported:

1. statistical analysis of signal states inside a spatial and temporal window (attenuation, noise, group and phase delays and corresponding rates);
2. composition of GNSS observations (ranges and phases) and corresponding estimation of the accuracy and availability of positioning;
3. extended composition of GNSS observations (ranges and phases) including the error generator model of the SSL and corresponding estimation of the accuracy and availability of positioning;
4. estimation of GNSS reliability by evaluation of several simulation runs with different spatial and temporal windows for typical static and dynamic applications

Depending on the selected operation mode and based on the defined global parameters the next steps are the initialization of each selected module, and if used, of the simulation subsystem SSL. At the end of simulation system set-up the geometric scenario (satellite constellation, user dynamics), the considered components (e.g. type and models for signal generation, propagation

channel, receiver hard- and firmware) and the desired results (e.g. signal states, navigation solution) are defined.

Only if all standard and selected optional modules are successfully initialized the corresponding simulation run can be started. During the simulation run the application simulation level generates the signal states at the receiver input (CNR, range and phase delays) and the *nominal* range and phase measurements. The signal states are used by the SSL to derive at each time stamp the corresponding *measuring errors* for these range and phase measurements. Because the calculation of range and phase errors of a specified system equipment is very intensive regarding computer time and memory, an error generator model is, therefore, used during the run of the end-to-end simulation. This model is derived from preliminary simulation runs of SSL using several sample sets of relevant signal states (including worst-case examples). The measuring errors delivered by the SSL are added to the nominal parts of range and phase (ASL). The thus composed range and phase observations of the tracked satellites are the database which is used for positioning. In addition, the system and satellite time behaviour and the orbit prediction error are generated by the ASL. They are used as error correction terms for the navigation solution. By comparison of the calculated and the specified position of one or several users, the accuracy, the availability and the reliability of positioning can be assessed. Both simulation levels are constructed modularly. Therefore, it is possible for further applications to substitute single modules by improved realizations or to compose extended simulation systems.

2.2. *Application simulation level (ASL)*

The operation mode of the ASL will be specified by selection of optional modules (Table I). This is a part of the specification of the universally valid parameter for the simulation realized by the dialog window shown in Figure 2. If the operation mode 1 is selected with enabled error generator, the necessary interface files for the signal simulation system are generated. Based on

Table I. Operation mode depending on selected modules.

| Module	Operation mode			
	1	2	3	4
Technical system specification	Standard	Standard	Standard	tbd
Satellite constellation	Standard	Standard	Standard	tbd
User constellation	Standard	Standard	Standard	tbd
Satellite antenna	Optional	Optional	Optional	tbd
Free space propagation	Optional	Standard	Standard	tbd
Ionosphere	Optional	Optional	Optional	tbd
Troposphere	Optional	Optional	Optional	tbd
Multipath/shadowing	Optional	Optional	Optional	tbd
Receiver antenna	Optional	Optional	Optional	tbd
Signal simulation system/error generator	Optional	Not usable	Standard	tbd
System/satellite time	Not usable	Optional	Optional	tbd
Orbit error generator	Not usable	Optional	Optional	tbd
Navigation solution	Not usable	Standard	Standard	tbd
Analyse unit signal states	Standard	Enable	Enable	tbd
Analyse unit positioning	Not usable	Optional	Optional	tbd
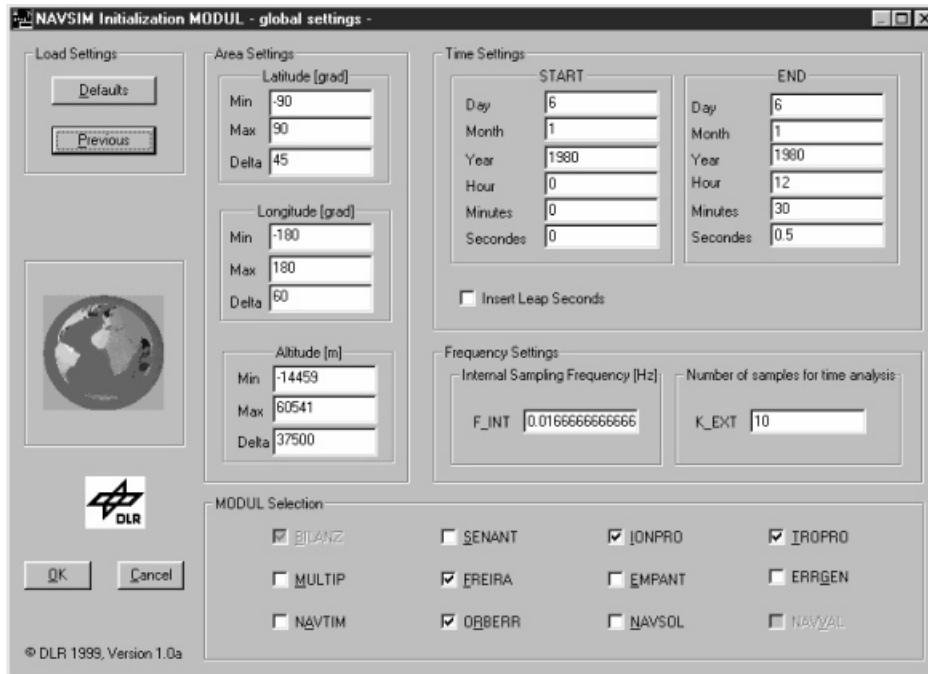
Figure 2. Dialog window for specification of universally valid simulation parameter.

these, preliminary signal simulations are realized by the signal simulation level (SSL) to deliver the necessary database for the error generator module used in operation mode 3. Depending on the desired goal in operation mode 4, several simulation runs (operation modes 1, 2 or 3) are analysed together to derive reliable evaluation of position accuracy or receiving conditions.

The other universally valid parameters (Figure 2) are the definition of the considered region, start and end point of simulation and the internal and external sampling frequencies. The internal sampling frequency defines the distance between two time stamps, where the signal states of all available links are calculated. With the definition of an external sampling frequency, which is smaller than or equal to the internal sampling frequency, temporary analysis of signal states and positioning accuracy with reduced data recording rate is possible.

After specification of the universally valid parameter the initialization of each selected module follows. The selection of models and the specification of necessary parameters are realized per module by one or more dialog windows similar to the specification of universally valid parameter. A further example is given for the composition of system and satellite clock generation (Figure 3). Each initialization step checks the value range, the parameter plausibility and the consistency before this initialization step is accepted. A simulation run can only be started if all necessary initialization files are marked as accepted.

During the simulation run at each time step the geometric available satellite signals for all users are determined. This is based on one or several satellite constellations described by a set of orbit parameters (almanacs or ephemerides in YUMA format) and on a user segment where the
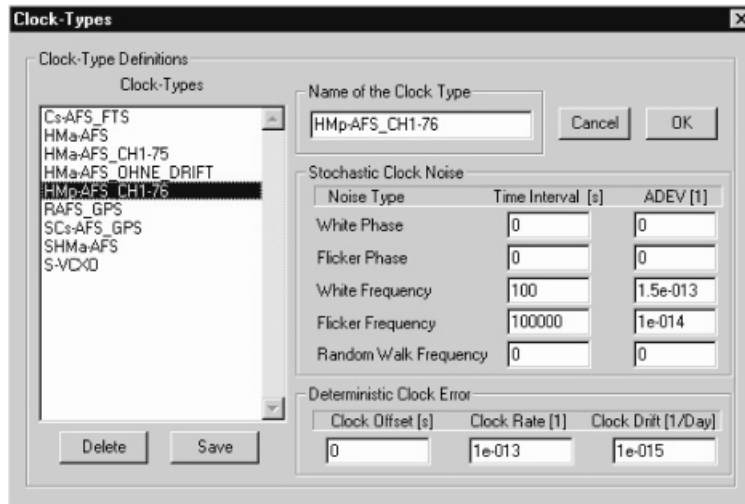
Figure 3. Initialization of clocks for generation of system and satellite time.

position and motion of the considered users is specified. With this concept any orbits of future satellite navigation systems can be created. After the satellite scenario thus having been defined, the user segment has to be determined. A certain range where the users are located must be specified. In this range the users can be uniformly distributed or special individual scenarios can also be created. In the case of the user-specific analysis a way trajectory will be assigned to each user. The trajectory will be described by a number of way points. On each way point a user is characterized by its velocity and acceleration. Of course, static users can also be simulated. These modules are necessary to construct the geometric scenario in the simulation time window.

For the available links, based on the well-known user's and satellite positions, the most important effects of signal propagation from the satellite to the receiver can be calculated with various implemented models and, therefore, with a different degree of accuracy. Influences are generally described by attenuation, noise, group, and phase delay per selected module (e.g. satellite/receiver antenna, free-space propagation, ionosphere, troposphere, multipath/ shadowing) at each time stamp.

To simulate the impact of regular and irregular ionospheric effects on radio propagation three models are implemented: IRI95 [1], BENT [2] and GIM. The first two models allow the reproduction of regular or mean ionospheric behaviour. The IRI95 model was implemented to provide a sophisticated ionospheric model from the ionospheric point of view. The BENT model has a very good runtime behaviour and an acceptable precision. GIM gives the basis for modelling amplitude fading and phase scintillation caused by small-scale electron density irregularities in the ionosphere. It is currently the only freely available model in Europe.

The troposphere module simulates delay, attenuation and thermal noise by the clear atmosphere and rain clouds. In order to simulate the delay of the clear troposphere independent of correction models which may be used in the receiver, the delay is computed by integration of the refractive index n along the curved path s from the receiver location to each satellite in view

including bending:

$$\Delta L_{i,j} = \int_{\text{Receiver}_i}^{\text{Satellite}_j} (n(s) - 1)\,\mathrm{d}s = 10^{-6} \int_{\text{Receiver}_i}^{\text{Satellite}_j} N(s)\,\mathrm{d}s \tag{1}$$

with

$$N = 10^6(n - 1) = 77.6\frac{P}{T} + 72\frac{e}{T} + 3.75 \times 10^5 \frac{e}{T^2} \tag{2}$$

[3]. For the vertical profiles of temperature T, pressure of dry air P and partial pressure of water vapour e the U.S.-standard atmosphere and other profiles for different regions and seasons [4] are implemented and can be selected manually or are automatically chosen depending on the user location and the date of simulation. The path attenuation is computed in a similar way as the delay by integration of the specific attenuation in dB/km, which is calculated as a function of height and frequency from the vertical profiles of T, P and e with equations given in Reference [5], along the curved path.

Additionally, rain effects can be included for a pre-selected system availability, either for a year or the so-called 'worst month', utilizing the ITU-R rain model [6], where the rain zone and the corresponding rain rate for a predefined user location and probability are automatically read from a file. Alternatively, a stratiform or cylindrical raincell model with user-defined rain rate and cell dimensions can be applied. If the rain rate and the rain path geometry are determined by one of these models, the path attenuations and delays for each user-to-satellite path are calculated by multiplication of the specific rain attenuation and specific delay per km with effective path lengths. The specific attenuation follows from regression coefficients delivered by the ITU-R rain model; for the computation of the specific delay the real part of the refractive index of rain is calculated with the MPM89-model [7].

The thermal noise temperature seen in the path direction is directly derived from the total path attenuation (rain plus clear atmosphere) applying the radiometric formula:

$$T_{\text{noise}} = T_{\text{m}}(1 - 10^{-0.1A}) + T_{\text{cosmos}}10^{-0.1A} \tag{3}$$

where A is the path attenuation in dB, T_{m} is the effective medium temperature (ca. 270–280 K) and T_{cosmos} is the cosmic background temperature (2.7 K). Finally, the noise temperature is converted to the noise power density by multiplication with the Boltzmann constant.

Based on the given radiation patterns of several satellite and receiver antennas their respective influence on signal strength and its capability to reduce multipath effects will be considered. Additionally, the variation of the antenna phase centre can be reproduced, which is essential to obtain accuracy in the mm range by evaluating the signal carrier phase.

Another disturbing effect is known as signal multipath propagation and results from the superposition of direct and indirect signal components, which come from reflections in the near environment of the antenna. The multipath can be described alternatively by deterministic or statistical models. In the ASL a deterministic model will be implemented, but is primarily used to improve the statistical models used in the SSL. The standard module 'Bilanz' superimposes the module parts to the CNR and the corresponding range and phase delays as signal states at the receiver input. From these an evaluation of receiving conditions can be done for a region, for a type of users or for a specific application of GNSS sensors.

If the position accuracy should be determined (operation mode 2 or 3), further modules are necessary to reproduce, on the one hand, the delivered navigation data (e.g. accuracy of predicted orbits and time-correction terms) and, on the other hand, the receiver quality (e.g. accuracy of detected range and phase observations and used navigation solution algorithm). Both have a significant influence on the attainable position accuracy: Because the simulation on the signal level needs high sampling rates pertaining to the signal description in the complex baseband, an error generator model will be implemented instead of the whole signal simulation system. The error generator is based on preliminary signal simulations results for samples of relevant and worst-case conditions derived for specific signal structures and receiver equipment.

The software also simulates the error effects caused by real physical clocks. For that the stochastic error of all used clocks, for the space segment as well as for the ground segment, are simulated by using the so-called power-law model. With this model, which calculates the error signal of all five stochastic clock noise types ['random walk frequency modulated noise (RWFM)', 'flicker frequency modulated noise (FFM)', 'white frequency modulated noise (WFM)', 'flicker phase modulated noise (FPM)' and 'white phase modulated noise (WPM)'], it is possible to simulate any kind of high precision clocks. Additionally, the deterministic clock errors like clock offset, frequency rate, and drift are modelled too.

The necessary parameters are calculated from the Allan variance information, which is normally available in the data sheet of a real clock. Thus, the user can individually simulate each existing real clock (according to its data sheet) or design new clocks. Furthermore, the program allows the user to choose clocks from a large list of predefined clocks, which contains different H-masers, rubidium, caesium and quartz clocks. With this, the user can individually define the clocks for each satellite and each ground station in the simulation.

With these simulated physical times of all clocks, the software calculates the system time with different algorithms. Furthermore, the clock correction coefficients *A0*, *A1*, *A2* will be calculated for each satellite by using a quadratic regression.

For the system time generation, the user can individually specify which clocks should be used. Additionally, the influence of each clock can be adjusted by a weighting factor. The first version of the simulator implements a weighted least squares and a Kalman filter-based algorithm [8] for the system time generation. Owing to the modular design of the simulator, it is easily possible to integrate other additional algorithms later. Thus, the effects of the clock errors of different clock types, as well as the algorithms used for calculating the system time, or the clock correction coefficients can be analysed.

Based on the composed range and phase observations for each user, the position and the corresponding accuracy is calculated instantaneously. For the simulation system two types of navigation solution are integrated for the time being. The first type of navigation algorithm is based on geometrical orientation of satellites and receiver [9]. First of all it searches the constellation of four satellites with the best GDOP value for a preliminary position of the receiver. In the case of simulation the origin position, which was set during the initialization of the simulation run, can be used for this. Then the following equation must be solved:

$$p_i = \sqrt{(x_i - x)^2 + (y_i - y)^2 + (z_i - z)^2} + c \cdot dt \qquad (4)$$

with p_i as the pseudoranges of the ith satellite with co-ordinates x_i, y_i, z_i to the receiver with co-ordinates x, y, z. Once the co-ordinates of the receiver have been computed, the receiver clock offset dt can be determined from (4) and the xDOP values are calculated to real receiver positions.

The second type of navigation algorithm [10] computes the receiver position as a solution of all satellites in view. Additional information like a preliminary receiver position are not necessary, but an iterative process has to be performed. In this case the index i goes from 1 up to the maximum number of visible satellites. Further types of navigation algorithm are planned to be implemented especially, in order to simulate the capability of dual or triple frequency positioning.

The gathered results can then be used to estimate the accuracy, the availability and the reliability of the considered GNSS for a region, for a type of users or for a specific application of GNSS sensors.

During a simulation the on-line derived results (signal states or position accuracy) are directed to evaluation modules, where a region or time-dependent analysis (e.g. mean values, RMS, distribution) can be realized and shown using various different graphic types like bar charts, plot charts, contour plots and histogram plots.

2.3. Signal simulation level (SSL)

Simulating a complete navigation system the large span of bandwidth causes numerous problems. The physical signal, for example, is sampled at 100 MHz. The atmospheric changes or satellite movements, on the other, change over the course of hours. To get a significant answer to questions such as 'what is the impact of ionospheric events on the accuracy of the navigation system?' the simulation would continue for years. This makes clear in which way the extremely high sampling frequency (100 MHz) causes problems in combination with the extremely slow changes of the other effects. Therefore, an efficient approach in terms of computational complexity has to be found.

2.3.1. Simulation of DLL and PLL.

A well-known approach for simulating digital systems taken from communication system simulations is the so-called 'sample-by-sample' approach. That means that the transmitter and the receiver are represented in the simulation according to their physical design (see Figure 4). Realizing a navigation system using this simulation approach the system calculates the pseudorange τ between the satellite and the receiver and the carrier phase φ (not depicted). A signal generator which represents the satellite in the simulation generates the navigation signal according to that determined pseudorange. The receiver (DLL) has to estimate this pseudorange. In contrast to communication systems it is not appropriate to assume ideal carrier or time synchronization. Within the simulation this becomes visible when digital samples
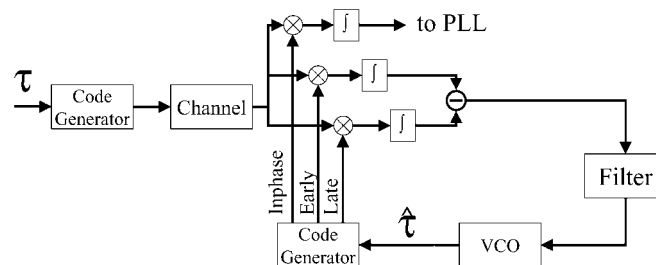
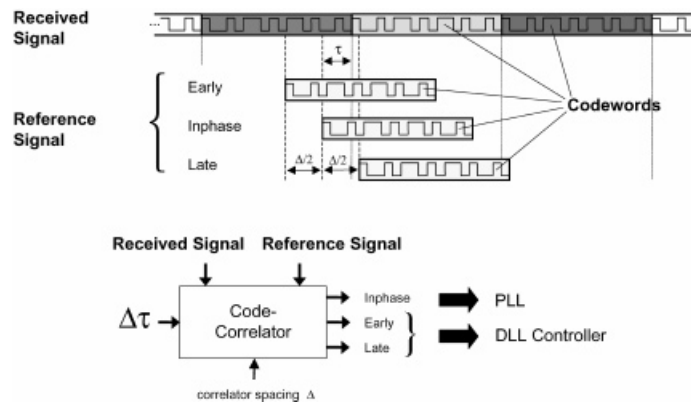Figure 4. 'Sample-by-sample' approach simulating navigation systems.

Figure 5. New, efficient approach.

with their time stamps are passed from the transmitter to the receiver. To avoid this 'unallowed help' the ideal sampling between satellite and receiver has to be destroyed. This can only be done by interpolation and resampling the signal which leads to high computational complexity. Furthermore, the code generator in the DLL must be able to synthesize any chip frequency – even those which are not devisors of the sampling frequency. Again interpolation and resampling comes into action. At this point it becomes evident that this approach is not capable of using sampling frequencies of 100 MHz.

In a new approach we model a combination of the signal generator in the satellite and in the receiver (DLL) to calculate the outputs of early, late and in-phase as depicted in Figure 5. Since in a simulation the real pseudorange between the satellite and the receiver is known, the difference $\Delta\tau$ between the pseudorange τ and the estimated pseudorange can be determined. The idea of this new approach is to calculate the output of the correlators early, late and in-phase directly with a much lower complexity. In this approach, interpolation has to be applied only once, asynchronous digital signal processing is avoided altogether.

Although the efficiency of this approach is much better than the 'sample-by-sample' approach it is still impossible to simulate days of real time using a sampling frequency of 100 MHz. Therefore, models have to be used to reach the goal of the overall navigation simulation system.

2.3.2. Characteristics of the error signals of DLL and PLL. All observations of DLL and PLL error signals result in a Gaussian distributed probability density function. Therefore, we assume a Gaussian power density function (PDF) for the error signal and parameterize it using the mean m and the variance σ. The time coherence between two samples is not independent and is represented in the spectrum of the error signal (see the example in Figure 6).

2.3.3. Modelling DLL and PLL noise in the simulator. The overall simulation is done in three steps:

- In the first step a 30 s period is simulated assuming a constant pseudorange between the satellite and the receiver.
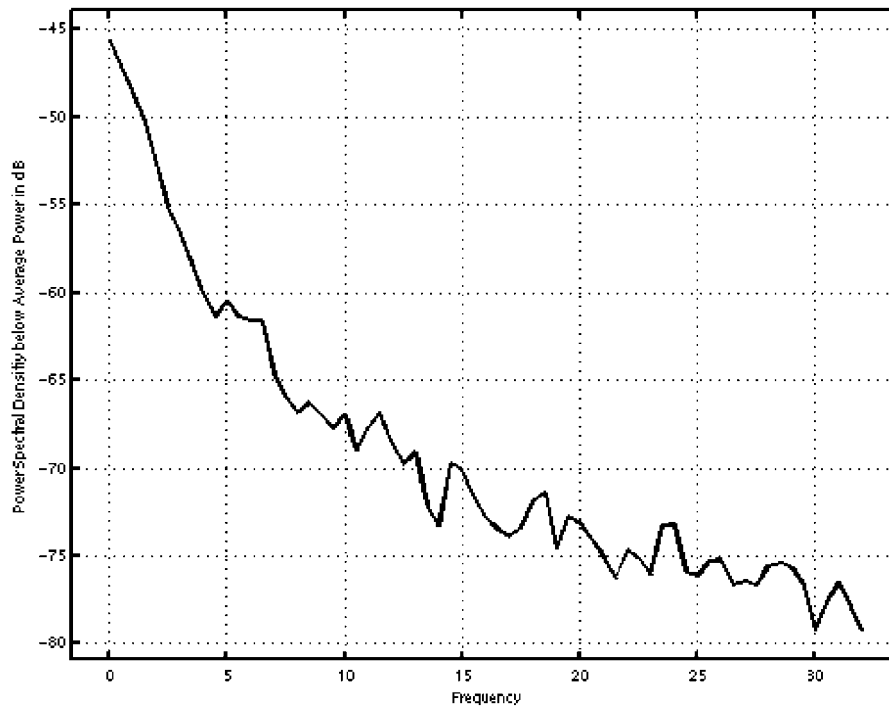
Figure 6. Power density spectrum of the DLL's error signal.

- In the second step the parameters mean value m, the variance σ and the spectrum are extracted.
- A model is used to generate the error signal of DLL and PLL.

The noise model of the receiver is build by a set of synthesizers (Figure 7). Each branch of these synthesizers represents a certain C/No. For example the first branch in Figure 7 represents a C/No of 30 dBHz. To generate the error signal a white Gaussian noise generator is used. Its signal is filtered using a filter according to the spectrum measured at a C/No of 30 dB Hz. Later on the noise is scaled using the measured variance and shifted to the measured mean m. To be able to simulate any C/No, interpolation between a set of these synthesizers is used for modelling the error signal.

2.3.4. Use in the overall simulator. Since the DLL and PLL are linear time-invariant (LTI) systems the LTI characteristic has to be modelled as well as the noise characteristic. The impulse response of the linearized loops can be calculated easily using the LTI theory. The response of a loop to a given pseudorange (or phase) can easily be calculated using a finite impulse response (FIR) filter. By simply adding the LTI responses and the noise error the effects of the LTI behaviour and the noise model are assumed to be independent, which is strictly speaking not correct; but simulations showed that they are nearly independent. The overall model is depicted in Figure 8.
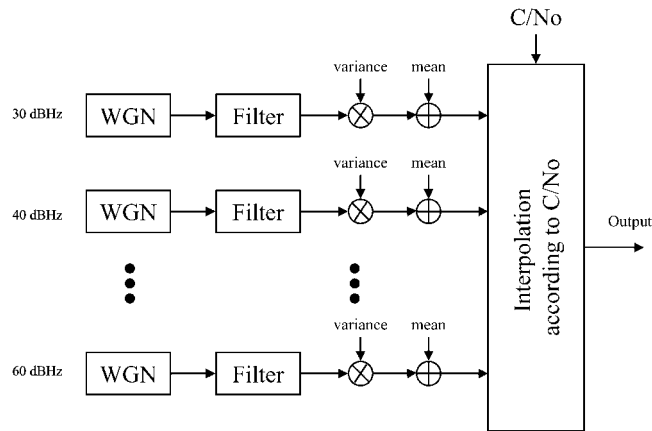
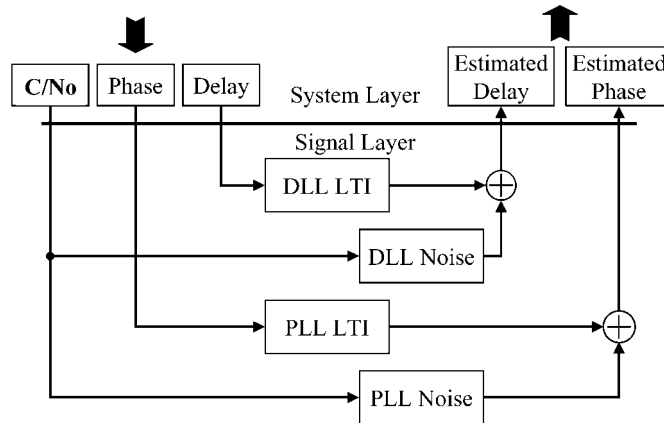Figure 7. Bank of synthesizers for emulating the error signal of an DLL/PLL caused by noise.

Figure 8. Overall model used for emulating the physical tracking loops in the receiver.

Using this three-step approach it is possible to overcome the large span of bandwidths and realize a system which is able to simulate effects on signal level as well as on system level.

3. EXAMPLES OF SIMULATION RESULTS

The project **NavSim** is responsible for the development of the software simulation system and will be finished at the end of the year 2000. Therefore, at this moment the full system capability is not reached. But several examples of partial simulation results are given to demonstrate the performance of the simulation system.
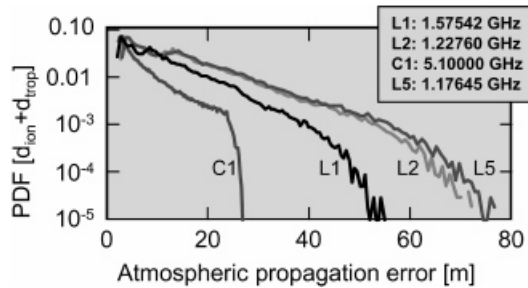
Figure 9. Distribution of ionospheric propagation error at 1 January 2000 (5° elevation mask).
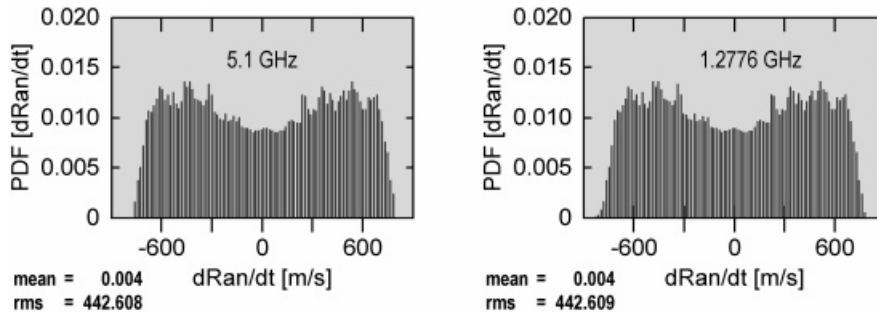

Figure 10. Range rate distribution at 1 January 2000 (5° elevation mask).

3.1. Estimation of receiving conditions

The composition of the signal states and the corresponding range and phase measurements is based on the calculation of the part of each technical component and natural impact.

The tropospheric transmission behaviour results in signal disturbances described by attenuation and noise terms and by code and phase delays. All derived terms are a function of the regional weather conditions and their daily and seasonal variations. The ionospheric influence on signal transmission depends on the solar activity, which is correlated with the electron density inside the ionosphere and the appearance of irregular effects (e.g. scintillation). In the year 2000 the 22nd solar cycle will reach its maximum and in consequence the ionospheric influences will drastically increase. The corresponding signal disturbances are rapid changes of signal amplitudes, code and phase delays and result in information losses and reduced tracking capabilities.

Different models integrated in the simulation system give the capability to reproduce these receiving conditions in the neutral atmosphere and the ionosphere. For demonstration 1st January in the year 2000 was chosen.

Assuming the GPS satellite constellation and considering the ionospheric, tropospheric and free-space propagation effects at 32 global well-distributed users the range rate distribution is shown in Figure 9. Though the mean range at 1.2276 GHz is ∼11 m, larger than in the case of 5.1 GHz, no significant changes can be observed in the range rate distribution. But looking at the distribution of atmospheric-induced propagation errors at existing and future GPS frequencies (Figure 10), the error range in the L-band is between two and three times that of the C-band. This
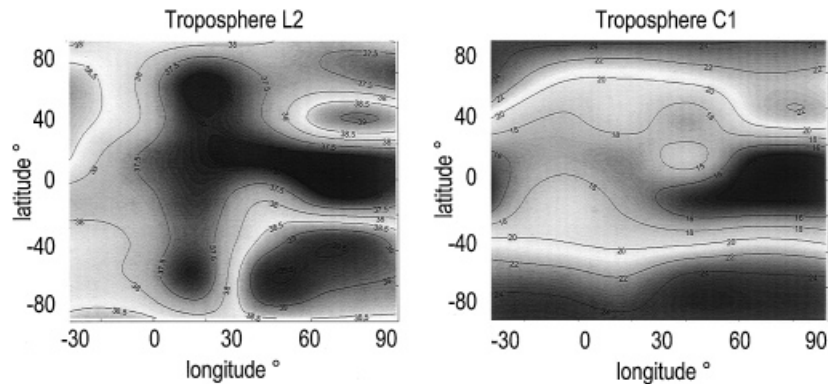
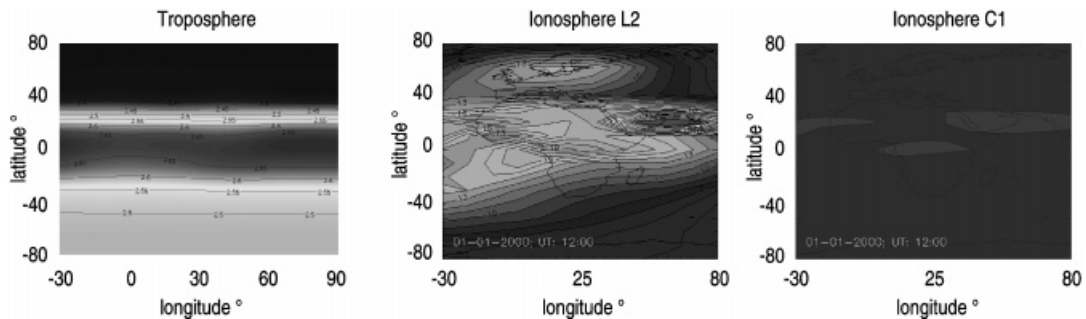Figure 11. Atmospheric induced CNR at 1 January 2000 at L2 and C1.

Figure 12. Vertical atmospheric propagation error observed at 1 January 2000 at 12:00.

effect is caused by the regular ionospheric behaviour described by the BENT model. This is shown in Figure 11, where the corresponding vertical propagation errors are shown separately for the ionosphere and troposphere (see Figure 12). The maximum of the tropospheric part is 2.65 m and is valid independent of frequency. At 1.2276 GHz the ionospheric part is up to 30 m, but at 5.1 GHz it is negligible.

A look at the atmospheric influence on CNR shows that the troposphere causes the main part in comparison with the regular ionosphere. Assuming a transmission power of 0 dB m shows that the gathered CNR is up to 20 dB lower than L2, if C1 is used.

Ionospheric influences on CNR are mainly a result of distortion effects, which occur only if signals with large bandwidths are tracked during the solar maximum with low elevation. This effect is lower than 2 dB in the L-band [11]. But if the ionosphere is disturbed and scintillations occur, then the ionosphere can cause short-term attenuation up to 30 dB. To reproduce this effect is a feature of the software simulation system planned for the end of the project.

Now consider the question: 'how large is the ionospheric-induced range error at tracked signals of the Internal Space Stations (ISS), if several carrier frequencies are allowed?' In comparison with GPS the propagation paths have higher dynamics, but the signals cross only the lower part of the

Table II. Ionospheric induced range error of global tracked signals of the ISS at 1 June 1991.

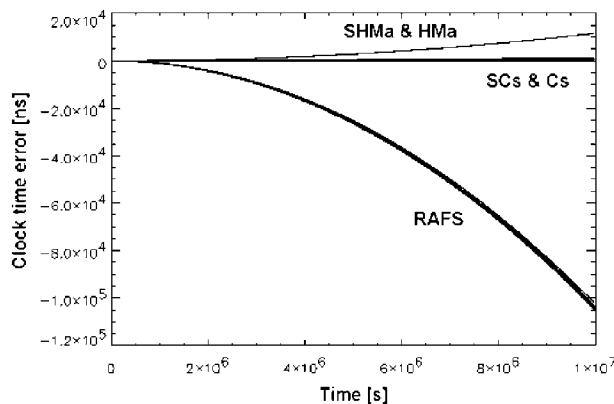| Frequency (GHz)	Mean (m)	rms (m)	Minimum–maximum (m)
0.4	100.868	72.094	3.344–382.162
1.4	8.234	5.885	0.273–31.197
2.25	3.188	2.278	0.105–12.078
13.475	0.089	0.064	0.003–0.337
14.703	0.075	0.053	0.002–0.283
15.85	0.064	0.046	0.002–0.243
17.1	0.055	0.039	0.002–0.209

Figure 13. Error signals of different clock types.

ionosphere. The observed range error was calculated using 48 global well-distributed stations and is shown in Table II for several frequencies.

Upon reaching the full capability of the simulation system, the CNR and the range and phase behaviour can be reproduced considering all propagation effects.

3.2. Satellite and system time behaviour

As described in Section 2.2 the software simulates the error signals of real physical clocks as well as the system time based on these simulation results. As an example the results of a scenario of 24 satellites (10 satellites with space proofed caesium clocks (SCs), 12 satellites with space proofed rubidium clocks (RAFS), 2 satellites with space proofed H-maser (SHMa)) and 6 ground stations (4 with caesium clocks (Cs), 2 with H-maser (HMa)) will be depicted in the next 4 figures.

The results of the simulated clock time error of all simulated clocks are shown in Figure 13 and the Allan standard deviation of these results are depicted in Figure 14. The typical behaviour of the different clock types are clearly visible.

With these clock signals a system time (STS), optimized for a sample interval of 4000 s, was calculated by using a weighted least-squares algorithm (see Figure 14). The time differences
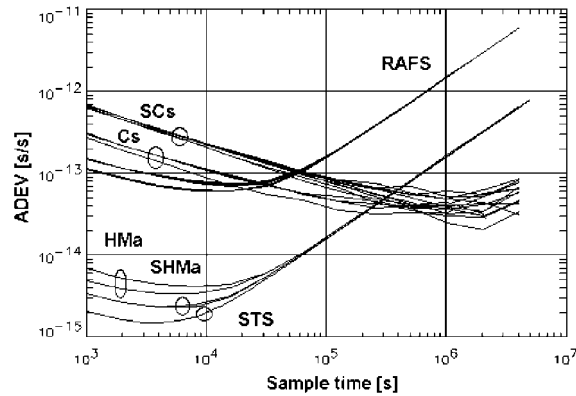
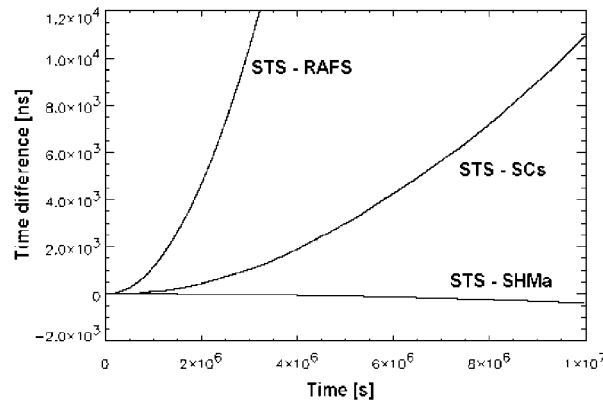Figure 14. Allan standard deviation of the clocks and the system time.

Figure 15. Time difference between satellite and system time.

between the calculated system time (STS) and the 3 different satellite clock types are plotted in Figure 15. The Allan standard deviations of these error signals are depicted in Figure 16.

3.3. Estimation of gathered positioning accuracy

If atmospheric propagation errors (ionosphere and troposphere) are not corrected in the raw data measurements, atmospheric-induced positioning errors occur. For 8 stations of the International Geodynamic Services (IGS) the daily mean errors are shown in Figure 17, if single frequency receiver are used. Depending on the used carrier frequency the mean error is of the order of 14–27 m. In this case the regional dependencies of the stations (southern, central and northern Europe) can be seen and results in variances of 2–3 m.
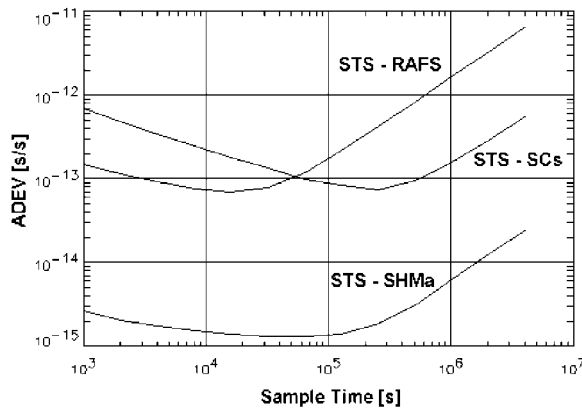
Figure 16. Allan standard deviations of the time difference between satellite and system time.
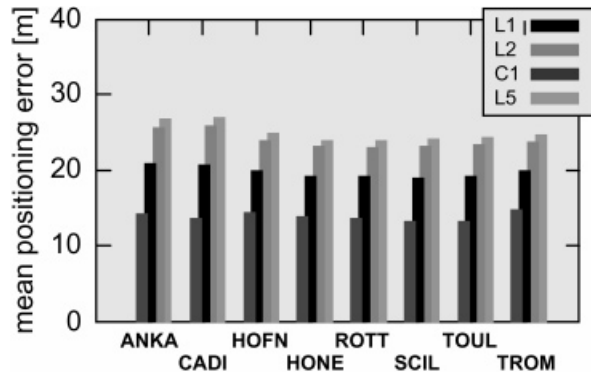

Figure 17. Atmospheric-induced positioning error observed at 1 January 2000 at several European IGS stations.

4. CONCLUSIONS

The software simulation system developed in the project NavSim is proposed as a suitable environment to develop and to evaluate models, algorithms and technical components in the navigation area under nearly realistic conditions. An example is the derived 'signal and equipment specific model of range and phase errors' based on the gathered data by partial simulations in the signal simulation level. For example, such models are important to lab-generate disturbed range and phase measurements in real time or to build up suitable signal simulators for receiver certification. To fulfil the requirements of an end-to-end simulation system the developed system consists of connected modules arranged in two simulation layers – the so-called signal simulation level and the application simulation level. This is necessary to achieve an acceptable computational complexity and to be open for further developments inside the simulator and its application as a tool.

ACKNOWLEDGEMENTS

REFERENCES

1. Bilitza (ed.). *International Reference Ionosphere* 1990, *NSSDC* 90-22. Greenbelt, Maryland, 1990.
2. Llewellyn SK et al. *Documentation and Description of the BENT Ionospheric model*, *AD*-772 733. Atlantic Science Corporation, prepared for Air Force Cambridge Research: distributed by NTIS, July 1973.
3. Damosso E, Stola L, Brussaard G. Characterisation of the 50–70 GHz band for space communication. *ESA Journal* 1983; **7**:25–43.
4. Smith EK, Weintraub S. The constants in the equation for atmospheric refractive index at radio frequencies. *Proceedings of IRE*, vol. 41, 1953; 1035–1037.
5. Ulaby FT, Moore RK, Fung AK. *Microwave Remote Sensing*, vol. 1. Addison-Wesley, Publishing Company: London, 1981; 261 ff.
6. ITU-R Recommendations PN.837-1 and 838. *PN Series Volume*: *Propagation in Non-Ionized Media*. *ITU-R*: Geneva, 1994.
7. Liebe HJ. MPM-An atmospheric millimeter wave propagation model. *International Journal of Infrared and Millimeter Waves* 1989; **10**(6):631–650.
8. Krämer R, Hahn J, Schmidt L. Results in GPS system time restitution with Kalman filters. 13*th European Frequency and Time Forum*, *EFTF*'99, 13-16.04.99, Besancon, France, 1999.
9. Kleusberg A. Die direkte Lösung des räumlichen Hyperbelschnitts. *Zeitschrift für Vermessungswesen* 1994; 188–192.
10. Bancroft S. An algebraic solution of the GPS equations. *IEEE Transactions on Aerospace and Electronic Systems* 1985; **AES-21**:56–59.
11. Engler E, Jungstand A, Bettac H-D. Ionospheric influence on satellite signals in the GHz range. *European Telemetry Conference*, *ETC*'98, 04-07.05.98, Garmisch-Partenkirchen, 1998.

AUTHORS' BIOGRAPHIES

Johann Furthner was born in Straubing, Germany, in 1964. He studied physics at the University of Regensburg, Germany from 1984–1990. In 1990 he received his degree in physics (Dipl. Phys.) with the Diploma thesis on coupling of two phase coupled Neodymium lasers to generate frequency variable and time synchronised pico second laser pulses. From 1990 to 1995 he was assistant at the Institute of Applied Physics of the University of Regensburg. In 1994 the degree of doctorate in physics was conferred to him at the Institute of Applied Physics of the University of Regensburg. His PhD thesis was on generating of time synchronised and frequency variable pico second laser pulses within Neodymium glass double branch laser. Since 1995 he has been working as a member of the research staff at the Institute of Radio Frequency Technology of the German Aerospace Center (DLR). He has worked on the development of a software simulator on signal chip level and application level for a second generation satellite navigation system (GNSS2-Galileo) in national and European projects.

Evelin Engler was born in Greiz, Germany, in 1960. She studied electrical engineering at the Technical University of Dresden, Germany from 1978–1983. In 1983 she received her degree (Dipl.-Ing). From 1983 to 1987 she was assistant at the Institute of Communications of the TU Dresden. For the scientific studies on the area 'Digital Modulation Techniques' the degree of doctorate was conferred on her in 1987. From 1987 to 1991 she has worked as a research staff member of the Institute of Cosmic Research at the Academy of Science and was involved in the verification of digital modulation techniques for the project 'OSFE' (Digital Data Transmission via Satellite TV Channels 'Moskwa') and in the mission support of 'OSFE'.

Since 1992 she has been working as a research staff at German Remote Data Centre of the German Aerospace Center (DLR). As the project leader of 'RAKO' she has taken part in the development of a real-time TEC station, which uses GPS measurements to describe the ionospheric state in Middle Europe by the so-called TEC maps. Further she has developed SW modules for the investigation of ionospheric induced non-linear distortion effects on signal transmission. Since 1997 she is the manager of the DLR project which deals with the development of an end-to-end SW simulation system for GNSS.

Alexander Steingaß was born in Mettmann, Germany, in 1969. He studied electrical engineering at the University of Ulm, Germany from 1989–1996. In 1996 he received a Dipl.-Ing. degree in electrical engineering working in his Diploma thesis on a new frame synchronisation approach. Since January 1997 he has been working as a member of research staff at the Institute for Communications Technology of the German Aerospace Center (DLR). He has designed the software architecture for a signal simulator for a second generation satellite navigation system (Galileo) in national and European projects.